European Congress on Computational Methods in Applied Sciences and Engineering
ECCOMAS 2004
P. Neittaanmäki, T. Rossi, K. Majava, and O. Pironneau (eds.)
R. Owen and M. Mikkola (assoc. eds.)
Jyväskylä, 24—28 July 2004

A FINITE ELEMENT CODE FOR STRUCTURAL COLLAPSE ANALYSES OF FRAMED STRUCTURES UNDER IMPACT LOADS

Daigoro Isobe* **and Kyaw Myo Lynn†**

* Institute of Engineering Mechanics and Systems, University of Tsukuba
1-1-1 Tennodai Tsukuba-shi, Ibaraki 305-8573, Japan
e-mail: isobe@kz.tsukuba.ac.jp, web page: http://www.kz.tsukuba.ac.jp/~isobe/

† Graduate school, University of Tsukuba
1-1-1 Tennodai Tsukuba-shi, Ibaraki 305-8573, Japan
e-mail: kyaw@kz.tsukuba.ac.jp

Key words: ASI-Gauss Technique, ASI Technique, Structural Collapse Analysis, Framed Structures, Impact Loads, Finite Element Method.

Abstract. *In this paper, we describe a new finite element code, which can be efficiently applied to structural collapse analyses of framed structures under impact loads. The code is developed by using the ASI-Gauss technique, a modified version of the formerly developed Adaptively Shifted Integration (ASI) technique for the linear Timoshenko beam element, which computes highly accurate elasto-plastic solutions even with the minimum number of elements per member. The ASI-Gauss technique gains still higher accuracy especially in elastic range, by placing the numerical integration points of the two consecutive elements forming an elastically deformed member in such a way that stresses and strains are evaluated at the Gaussian integration points of the two-element member. Moreover, the technique can be used to express member fracture, by shifting the numerical integration point to an appropriate position and by releasing the resultant forces in the element simultaneously. An impact phenomenon between structures is expressed by means of contacts between the elements involved, and the elemental contact algorithm is verified from the point of conservation of energy. Impact analyses considering member fracture with different sets of parameters are performed on a high-rise framed structure collided by a small aircraft. From the results obtained, we can observe propagation of impact loads and shock waves in the framed structure. Also, the results indicate that the larger the pre-impact kinetic energy, the larger the impact damage. In the cases of the same pre-impact kinetic energy, slight differences are observed when the parameters of the aircraft are varied. Moreover, soon after impact, tensile stresses are observed in the columns that were compressed by dead loads before impact.*

1 INTRODUCTION

The progressive collapse of World Trade Center towers in New York, USA revealed the structural vulnerability of tall steel buildings to the impact of a fast moving object. Technical investigations are necessary to clarify the technical conditions that contributed to the progressive collapse and to improve the ways buildings are designed, constructed, maintained and used. Generally, numerical simulation is considered to be one of the means to investigate such problems.

Advancements in computational technology have helped the development of various numerical analysis methods and some of them have been applied to analyze dynamic behaviors with strong nonlinearities and discontinuities. The Distinct Element Method (DEM) [1] follows the discontinuum approach, that is, the analytical model is formed by a number of distinct interacting general-shaped elements to simulate the perfectly discrete behavior. The Discontinuous Deformation Analysis (DDA) [2] models a discontinuous material as a system of individually deformable blocks that move independently without interpenetration. DDA is known to be able to cope with large deformations and strong discontinuities. The Applied Element Method (AEM) [3], which can predict crack initiation and propagation in the material and can also follow the total behavior from zero loading to complete collapse, has also been developed and applied to detailed nonlinear analysis of reinforced concrete structures. However, the above-mentioned discrete numerical methods are computationally intensive and need detailed modeling. Therefore, they are suitable only for detailed analyses of either two-dimensional or small three-dimensional models.

On the other hand, the Finite Element Method (FEM), which is based on continuum material equations, has been successfully applied to a wide range of engineering problems including structural analyses of large-scale structures. However, the FEM is generally limited to analyses of relatively small displacements and it needs complicated modifications to apply to strongly nonlinear and discontinuous problems. The main objective of this study is to develop a finite element code, which can simulate dynamic behaviors with strong nonlinearities and discontinuities and is efficiently applicable to impact collapse analyses of framed structures.

Toi and Isobe developed the Adaptively Shifted Integration (ASI) technique [4,5] for the linear Timoshenko beam and the Euler-Bernoulli beam elements, which can be easily implemented into the existing finite element codes. In this technique, the numerical integration point is shifted immediately after the occurrence of a fully plastic section in the element so that a plastic hinge is formed exactly at that section. As a result, the ASI technique gives more precise elasto-plastic solutions than the conventional schemes, and has become able to simulate dynamic behaviors with strong nonlinearities by using only a small number of elements for a member. Structurally discontinuous problems have also become easily handled, by shifting the numerical integration point of the linear Timoshenko beam element to an appropriate position, and by releasing the resultant forces in the element simultaneously [6,7]. However, when the number of elements per member is very small, it still lacks accuracy in the elastic range compared to the converged solution, due to the low-degree displacement function of the linear Timoshenko beam element.

In this study, the ASI technique using the linear Timoshenko beam element is modified into the ASI-Gauss technique to improve its accuracy especially in elastic range. It is handled by placing the numerical integration points of the two consecutive elements forming an elastically deformed member in such a way that stresses and strains are evaluated at the Gaussian integration points of the two-element member, where the accuracy of bending deformation is mathematically guaranteed for two-point integration. The numerical integration points are adaptively shifted according to the change in material property (elasto-plasticity) of the member. The validity of the ASI-Gauss technique is verified, in this paper, by comparing with the ASI technique and the conventional scheme. The impact phenomenon between structures is expressed by means of contacts between the elements involved, and the elemental contact algorithm is verified from the point of conservation of energy. Generally, it is difficult to determine the loads resulted in the structures due to an impact, and applying impact loads to an analytical model in the form of nodal forces may not well simulate the impact phenomenon. But by using the elemental contact algorithm, the phenomenon can be suitably expressed even when the parameters for the colliding structure are varied. Dynamic collapse analyses considering member fracture and elemental contact are performed to simulate the impact of a small aircraft into a ten-storied steel framed structure, and observations are made to evaluate the influence of mass, velocity and size of the aircraft on the impact damage.

2 METHODS

In this section, the ASI technique using the linear Timoshenko beam element is summarized. It is followed by the explanation on the newly proposed ASI-Gauss technique, and the algorithms considering member fracture and elemental contact.

2.1 Adaptively Shifted Integration (ASI) technique

Elasto-plastic analyses of framed structures using the linear Timoshenko beam element are based on the following incremental form of the principle of virtual work:

$$\delta \mathrm{V} - \delta \mathrm{W} = \int_{-L/2}^{L/2} \{\delta \Delta \varepsilon\}^T \{\Delta \sigma\} dz - \{\delta \Delta u\}^T \{\Delta f\} = 0 \tag{1}$$

where V and W are the internal work and the external work, {Δε}, {Δσ}, {Δu}, and {Δf} are the generalized strain increment vector, the generalized stress (resultant force) increment

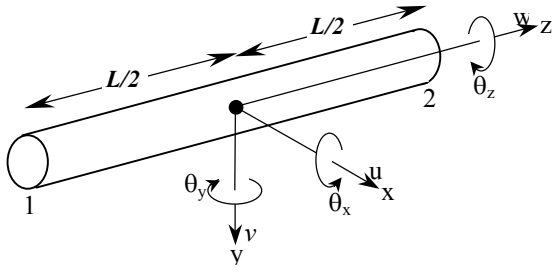

Figure 1: Definitions of local coordinates and displacements.

vector, the nodal displacement increment vector and the external force increment vector, respectively. The symbols δ and Δ denote variation and increment. The local coordinates, nodal numbers and displacement components (u, v, w, θ_x, θ_y, θ_z) are shown in Fig.1.

The relation between the generalized strain increment and nodal displacement increment vectors are given by the following equation:

$$\{\Delta\varepsilon(r)\} = [B(s)]\{\Delta u\} \tag{2}$$

where [B(s)] is the generalized strain-nodal displacement matrix. **s** is the location of the numerical integration point and **r** the location where stresses and strains are actually evaluated. We refer **r** as the stress evaluation point later in this paper. **s** is a non-dimensional quantity, which is defined as z/(L/2) where L is the length of the element. **s** takes a value between –1 and 1. It should be noted here that the linear Timoshenko beam element uses one-point integration to avoid shear locking.

When the element behaves elastically, the relation between resultant force increment vector and generalized strain increment vector is given by the following equation:

$$\{\Delta\sigma(r)\} = [D_e(r)]\{\Delta\varepsilon(r)\} \tag{3}$$

where $[D_e]$ is the stress-strain matrix for elastic deformation. Substitution of Eqs. (2) and (3) into Eq. (1) leads to the following form of elemental stiffness matrix:

$$[K] = L[B(s)]^T [D_e(r)][B(s)] \tag{4}$$

In the ASI technique, numerical integration points are shifted immediately after the formation of a fully plastic section in the element in order to form a plastic hinge exactly at that section. When a plastic hinge is judged to be unloaded, the corresponding numerical integration point is shifted back to its normal position. Here, the normal position means the location where the numerical integration point is placed when the element acts elastically.

Figure 2 shows a linear Timoshenko beam element and its physical equivalence to a rigid-body-spring-model (RBSM). As shown in the figure, the relationship between the locations of the numerical integration point and the stress evaluation point where a plastic hinge is actually formed is expressed as follows:

$$r_1 = -s_1 \tag{5}$$

When the entire region of an element behaves elastically, the numerical integration point is placed at the midpoint of the element ($\mathbf{s_1}$=0) which gives $\mathbf{r_1}$=0 from Eq. (5) in this case. The elemental stiffness matrix for the element, the generalized strain increment vector and the resultant force increment are calculated as follows:

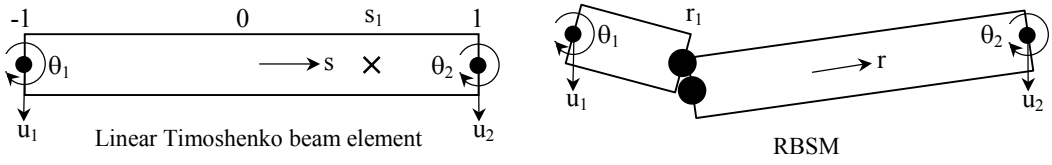

Figure 2: Linear Timoshenko beam element and its physical equivalent.

$$[K] = L[B(0)]^T [D_e(0)][B(0)] \tag{6a}$$

$$\{\Delta\varepsilon(0)\} = [B(0)]\{\Delta u\} \tag{6b}$$

$$\{\Delta\sigma(0)\} = [D_e(0)]\{\Delta\varepsilon(0)\} \tag{6c}$$

The resultant forces calculated from Eq. (6c) are physically those at the midpoint of the element.

According to the elementary beam theory, the relations between the bending moments and shear forces are given as follows:

$$V_x = -\frac{dM_y}{dz} \tag{7a}$$

$$V_y = -\frac{dM_x}{dz} \tag{7b}$$

Here, M_x and M_y are the bending moments around x- and y-axes while V_x and V_y are the shear forces along x- and y- axes. Thus the distributions of the bending moment increments in an elastically deformed element are determined by the following approximations:

$$\Delta M_x(s) = \Delta M_x(0) - \Delta V_y(0)\frac{Ls}{2} \tag{8a}$$

$$\Delta M_y(s) = \Delta M_y(0) - \Delta V_x(0)\frac{Ls}{2} \tag{8b}$$

The above equations show that the bending moments are subject to a linear change in an element and are likely to take the maximum value on either ends ($\mathbf{s}=\pm 1$). As other resultant forces have constant values in the element, a fully-plastic state can be determined with an yield function by comparing the calculated distributions from Eqs. (8).

After the formation of a fully plastic section, the numerical integration point is shifted immediately to a new point ($\mathbf{s_1} = -\mathbf{r_1}$). For instance, if a fully plastic section occurs at the right end of an element ($\mathbf{r_1}=1$), the numerical integration point is shifted to the left end ($\mathbf{s_1} = -1$) and vice versa. In this case, the elemental stiffness matrix, the generalized strain and resultant force increment vectors are given as follows:

$$[K] = L[B(s_1)]^T [D_p(r_1)][B(s_1)] \tag{9a}$$

$$\{\Delta\varepsilon(r_1)\} = [B(s_1)]\{\Delta u\} \tag{9b}$$

$$\{\Delta\sigma(r_1)\} = [D_p(r_1)]\{\Delta\varepsilon(r_1)\} \tag{9c}$$

Here, $[D_p]$ is the stress-strain matrix for plastic deformation. It is determined by the plastic flow theory using the following form of yield function:

$$f_y(\sigma(r)) - 1 = 0 \tag{10}$$

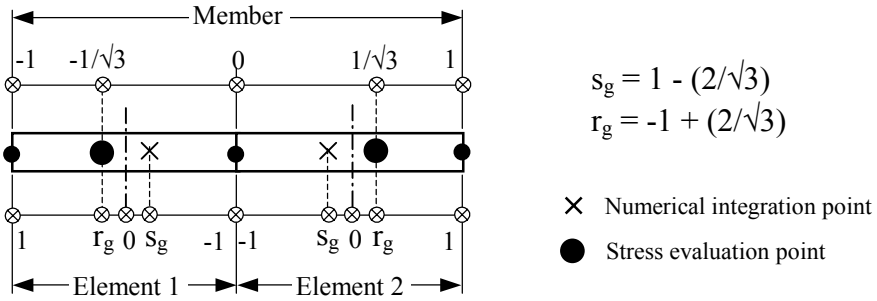

Figure 3: Locations of numerical integration and stress evaluation points in ASI-Gauss technique.

2.2 ASI-Gauss technique

In this paper, we propose the ASI-Gauss technique for elasto-plastic collapse analyses of framed structures using the linear Timoshenko beam element. As in the ASI technique, the numerical integration point is shifted immediately after the formation of a plastic hinge and it is shifted back to its normal position when the element is unloaded. The main difference between the ASI and the ASI-Gauss techniques lies in their normal positions of the numerical integration points.

The relationship between the locations of the numerical integration point and the stress evaluation point is expressed as follows:

$$r_g = -s_g \tag{11}$$

When the entire region of an element behaves elastically, the numerical integration point is located at ($\mathbf{s_1}$=$\mathbf{s_g}$). As shown in Fig.3, the normal position of the numerical integration point in the ASI-Gauss technique is $\mathbf{s_g}$=1−(2/√3) and the stress evaluation point is $\mathbf{r_g}$= −$\mathbf{s_g}$ = −1+(2/√3). The two stress evaluation points coincide with Gaussian integration points of the member. This means that stresses and strains are evaluated at Gaussian integration points when the element behaves elastically. Gaussian integration points are known to be optimal for two-point integration and the accuracy of bending deformation is mathematically guaranteed [8]. In this case, the elemental stiffness matrix, the generalized strain and resultant force increment vectors are given as follows:

$$[K] = L[B(s_g)]^T [D_e(r_g)][B(s_g)] \tag{12a}$$

$$\{\Delta\varepsilon(r_g)\} = [B(s_g)]\{\Delta u\} \tag{12b}$$

$$\{\Delta\sigma(r_g)\} = [D_e(r_g)]\{\Delta\varepsilon(r_g)\} \tag{12c}$$

The distributions of the bending moment increments in an elastically deformed element are determined by the following approximations:

$$\Delta M_x(s) = \Delta M_x(s_g) - \Delta V_y(s_g)\frac{L}{2}(s + s_g) \tag{13a}$$

$$\Delta M_y(s) = \Delta M_y(s_g) - \Delta V_x(s_g)\frac{L}{2}(s + s_g) \tag{13b}$$

Immediately after the occurrence of a fully plastic section, the numerical integration point is shifted to a new point ($\mathbf{s_1}= -\mathbf{r_1}$) as in the ASI technique. For instance, if a fully plastic section occurs at the right end of an element ($\mathbf{r_1}$=1), the numerical integration point is shifted to the left end ($\mathbf{s_1}= -1$) and vice versa. The elemental stiffness matrix, the generalized strain vector and resultant force increment vector are given by Eqs. (9a), (9b) and (9c). It is to be noted here, that in this case, the numerical integration point of the adjacent element forming the same member is shifted back to the midpoint of the element where its accuracy is guaranteed against one-point integration. If the plastic hinge is judged to be unloaded, both numerical integration points in the two-element member are, again, shifted to the locations according to Fig.3. In other words, the locations of numerical integration points are adaptively shifted according to the change in material property (elasto-plasticity) of the member.

The yield function assumed in this study is expressed by the following equation:

$$f_y \equiv \left(\frac{M_x}{M_{x0}}\right)^2 + \left(\frac{M_y}{M_{y0}}\right)^2 + \left(\frac{N}{N_0}\right)^2 + \left(\frac{M_z}{M_{z0}}\right)^2 = 1 \tag{14}$$

Here, M_x, M_y, N and M_z are the bending moments around x- and y- axes, the axial force and the torsional moment, respectively. Those with the subscript 0 are the values that cause a fully plastic section in an element when they act on the cross-section independently. The effect of shear forces is neglected in the yield function.

The dynamic collapse analysis is made possible by adding inertial force terms to the quasi-static computational procedure. That is, the following equation for the complete system is integrated by an appropriate time integration scheme:

$$[M]\{\ddot{u}\}_{t+\Delta t} + [C]\{\dot{u}\}_{t+\Delta t} + [K]\{\Delta u\} = \{F\}_{t+\Delta t} - \{R\}_t \tag{15}$$

Here, [M] is the total mass matrix, [C] the total damping matrix, [K] the total stiffness matrix, $\{F\}_{t+\Delta t}$ the nodal external force increment vector at t+Δt, $\{R\}_t$ the nodal internal force increment vector at t. $\{\ddot{u}\}_{t+\Delta t}$, $\{\dot{u}\}_{t+\Delta t}$ and $\{\Delta u\}$ are the nodal acceleration, velocity and displacement increment vector at t+Δt. In this study, we use consistent mass as an elemental mass matrix which is assumed to be unaffected by the shifting of numerical integration points. Newmark's β method [9] is used as a numerical integration scheme for Eq. (15), and conjugate gradient (CG) method is used as a solver to reduce the need of memory resources.

2.3 Algorithm considering member fracture

A plastic hinge is likely to occur before it develops to a member fracture, and the plastic hinge is expressed by shifting the numerical integration point to the opposite end of the fully-plastic section. Accordingly, the numerical integration point of the adjacent element forming the same member is shifted back to its midpoint where it is appropriate for one-point integration. Figure 4 shows the locations of numerical integration points for each stage in the

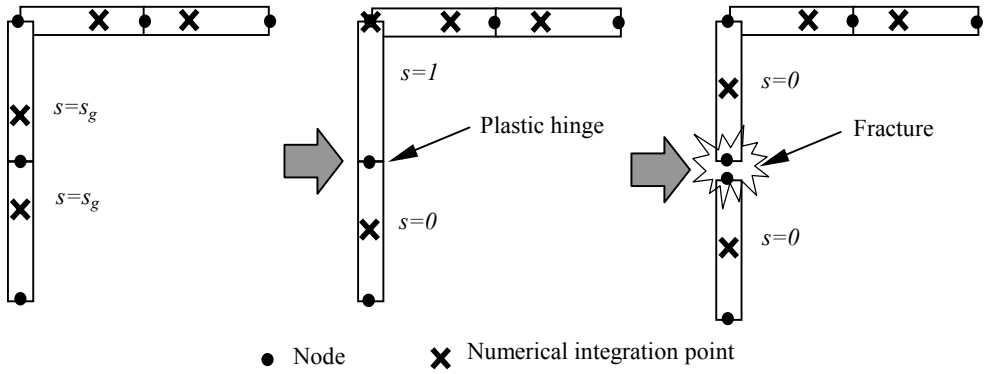

Figure 4: ASI-Gauss technique dealing with member fracture.

ASI-Gauss technique. A member fracture is determined, in this study, by examining axial and bending strains in two elements forming a member, using the following conditions.

$$\left(\frac{\kappa_x}{\kappa_{fx}}\right)-1\geq 0,\ \left(\frac{\kappa_y}{\kappa_{fy}}\right)-1\geq 0,\ \left(\frac{\varepsilon_z}{\varepsilon_{fz}}\right)-1\geq 0 \tag{16}$$

Here, κ_x, κ_y, ε_z, κ_{fx}, κ_{fy} and ε_{fz} are the bending strains around x- and y- axes, the axial strain and the critical values for each strain, respectively. When fracture is judged to occur, a new node is created at the fractured section and the numerical integration point of the element is shifted back to its midpoint. Resultant forces exerting at the fractured section are released instantly at the next step after fracture has occurred. The nodal mass is equally redistributed at each separated node after the step.

2.4 Algorithm considering elemental contact

Generally, it is difficult to determine the loads resulted in the structures due to an impact. Applying impact loads to the model in the form of nodal forces may not well simulate the impact phenomenon. Thus, the impact phenomenon is expressed, in this paper, by means of contact between the elements involved. Elemental contact algorithm is also useful to simulate fractured elements colliding with other elements, and to consider the variation of parameters of the colliding structure.

Contact determination is done by examining the following two factors: (i) the distance between the approaching element and the another one, (ii) the condition under which all four nodal points lie on the same plane. Figure 5 shows the geometric relation in the contact determination. Using the coordinates of the nodal points of the colliding element; $A_1(x_{c1},y_{c1},z_{c1})$, $A_2(x_{c2},y_{c2},z_{c2})$, and another element E_i; $B_{i1}(x_{i1},y_{i1},z_{i1})$, $B_{i2}(x_{i2},y_{i2},z_{i2})$, the condition under which all four nodal points lie on the same plane can be expressed as follows:

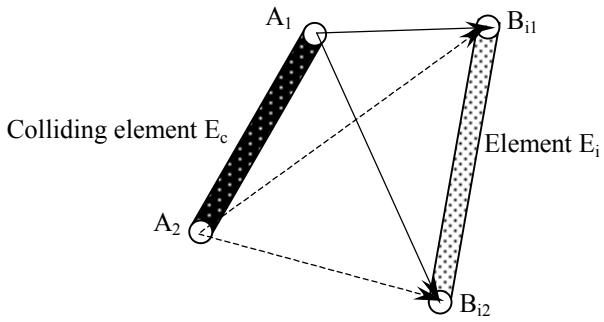

Figure 5: Geometric relation in the determination of elemental contact.

$$\begin{aligned} f(x,y,z) \equiv & \{(y_{i1}-y_{c2})(z_{i2}-z_{c2})-(y_{i2}-y_{c2})(z_{i1}-z_{c2})\}(x_{c1}-x_{c2})+ \\ & \{(x_{i2}-x_{c2})(z_{i1}-z_{c2})-(x_{i1}-x_{c2})(z_{i2}-z_{c2})\}(y_{c1}-y_{c2})+ \\ & \{(x_{i1}-x_{c2})(y_{i2}-y_{c2})-(x_{i2}-x_{c2})(y_{i1}-y_{c2})\}(z_{c1}-z_{c2})=0 \end{aligned} \tag{17}$$

When two elements lie on the same plane and exist within a specific distance from each other as calculated by the following equation, they are assumed to be in contact:

$$\left|\overline{A_1B_{i1}}\right|+\left|\overline{A_1B_{i2}}\right|+\left|\overline{A_2B_{i1}}\right|+\left|\overline{A_2B_{i2}}\right| \le C_l\left(L_c+L_i\right) \tag{18}$$

Here, $\left|\overline{A_1B_{i1}}\right|$, $\left|\overline{A_1B_{i2}}\right|$, $\left|\overline{A_2B_{i1}}\right|$, $\left|\overline{A_2B_{i2}}\right|$ are the distances between the four nodal points and L_c, L_i the lengths of colliding element E_c and the element E_i, respectively. C_l is the coefficient concerning contact length and a value of 1.8 is used throughout this paper.

For the elements that do not lie on the same plane but exist within a certain distance specified by Eq. (18), another condition is given as expressed by the following equation, which assumes that the elements nearly form a plane:

$$f(x,y,z) \le C_f \tag{19}$$

C_f is a coefficient expressing the degree of planarity, which is fixed by considering the

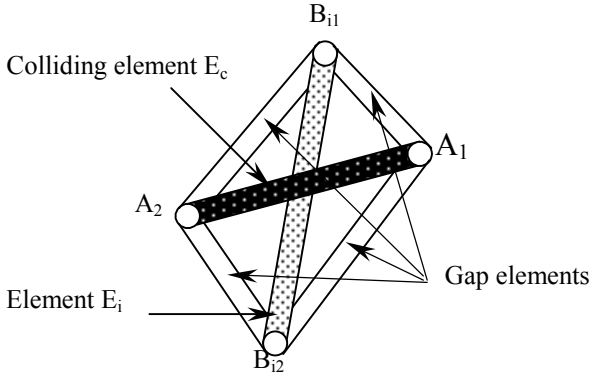

Figure 6: Four gap elements binding the two elements in contact.

sectional properties of constituent members. In this paper, a value of $3.0\text{x}10^{-4}$ m^3 is used for C_f. Contact determination is skipped for the elements that are not approaching each other. When two elements are determined to be in contact, they are bound with a total of four gap elements as shown in Fig.6. Gap elements are assumed to have the same geometric and material properties as the elements in contact. In the case of contact, impact force is delivered through these gap elements to the connecting elements. After certain time of contact, the gap elements are removed from the analytical model. In this paper, the binding time is set to 0.5 ms. It is assumed that no energy loss takes place during the impact.

3 NUMERICAL EXAMPLES

In this section, the results of the elasto-plastic collapse analyses using a simple space frame, which is loaded both statically and dynamically, are discussed. In the analyses, we use the following three schemes in order to verify the accuracy of the newly proposed ASI-Gauss technique: (a) conventional scheme in which the numerical integration point of each element is fixed at its midpoint; (b) the ASI technique; (c) the ASI-Gauss technique. Moreover, the algorithm considering elemental contact is verified from the point of conservation of energy by carrying out an impact analysis of a two-beam model.

3.1 Elasto-plastic collapse analysis of a space frame

Figure 7 shows the analyzed space frame with its dimensions, geometric properties and material constants. As shown in the figure, the frame is fixed at its lower ends and a static horizontal load is applied to its upper left corner. Members are subdivided into elements according to the numbers specified in the legends of the figures. As large deformations are not expected, the total Lagrangian formulation (TLF) is used in the analyses.

Figure 8 shows the results of the elasto-plastic analyses under static loading. As for the conventional scheme, convergence is extremely slow. The ASI technique shows better convergence, since the numerical integration points are shifted to form plastic hinges at appropriate locations. However, it still shows slow convergence in the elastic range, due to the low-degree displacement function of the element. On the other hand, the ASI-Gauss technique shows that just two-element modeling is needed to obtain the converged solution in the elasto-plastic analysis.

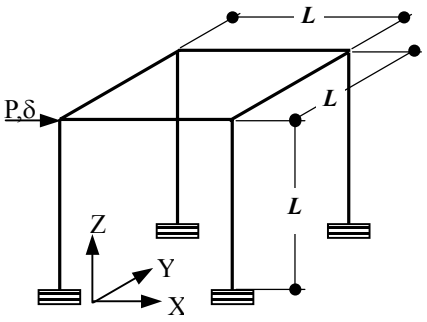

$L = 2.00$ m, $A = 2.50\times10^{-3}$ m^2

$I_x = I_y = 5.21\times10^{-7}$ m^4

$\rho = 7900$ kg/m^3, $E = 206$ GPa

$\upsilon = 0.3$, $\sigma_y = 245$ MPa

$M_{x0} \equiv M_{y0} = 7.66\times10^{3}$ Nm

$N_0 = 6.13\times10^{5}$ N

$M_{z0} = 1.12\times10^{5}$ Nm

Figure 7: Analyzed space frame model.

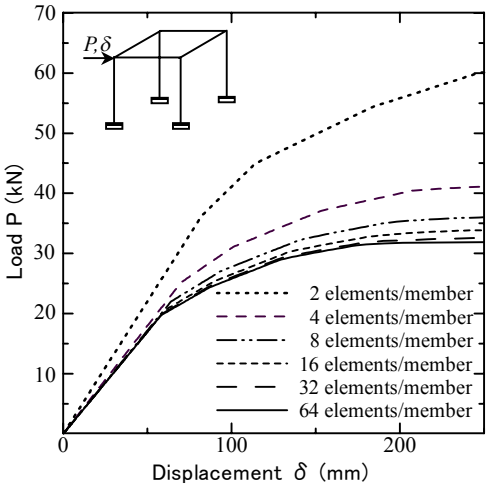

(a) Conventional scheme

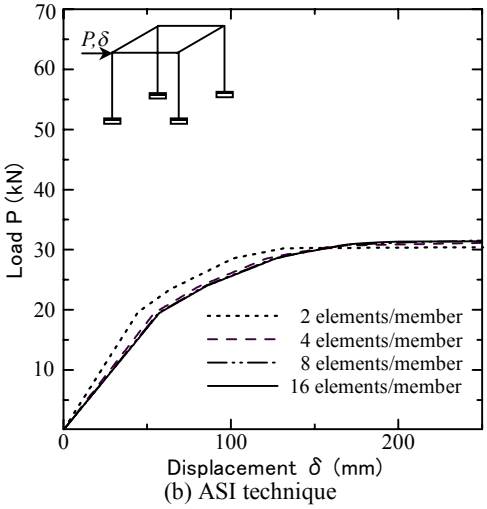

(b) ASI technique

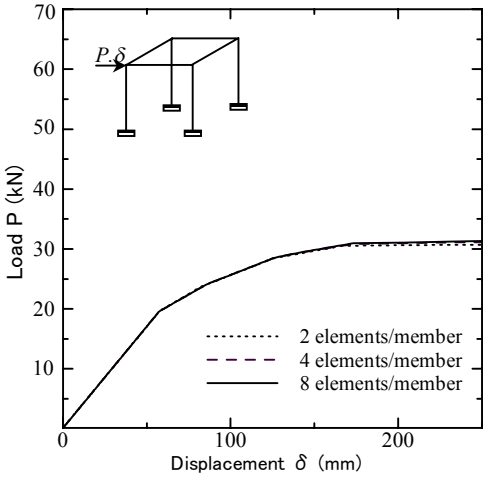

(c) ASI-Gauss technique

Figure 8: Elasto-plastic collapse analysis.

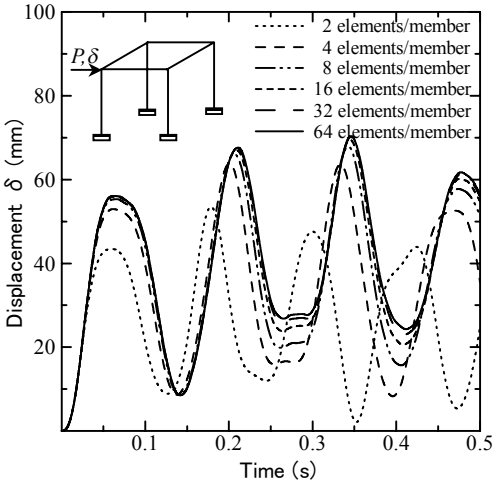

(a) Conventional scheme

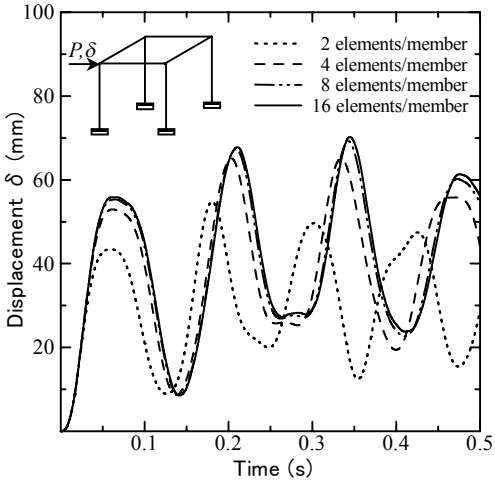

(b) ASI technique

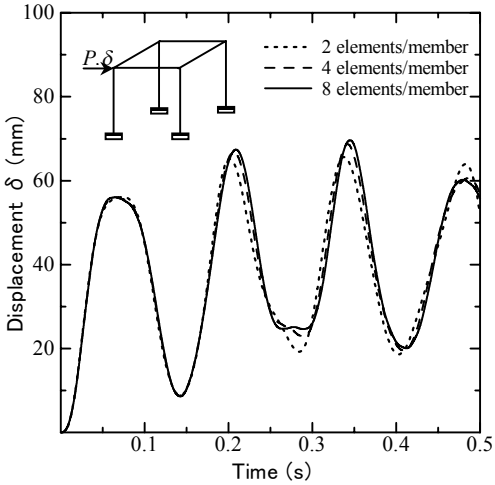

(c) ASI-Gauss technique

Figure 9: Elasto-plastic response analysis.

3.2 Elasto-plastic response analysis of a space frame

In the analyses subjected under dynamic loading, the time increment Δt is set to 0.05 ms and the same model shown in Fig.7 is used. A step load of 12 kN is applied for a total of 100 steps (5 ms). Damping effect is not considered in the analysis.

Figure 9 shows the results of the elasto-plastic response analyses under dynamic loading. As in the analyses described in the previous section, the conventional scheme shows very slow convergence and at least sixteen-element modeling is necessary to obtain the converged solution in the analysis. The ASI technique gives comparatively better results than the conventional scheme. However, when it comes to the model that uses only two elements per member, poor convergence is seen and the vibration mode is much different from that of the converged solution. On the other hand, the ASI-Gauss technique shows very fast convergence in the result and nearly converged solutions are obtained even when the number of elements per member is two.

From the above analyses, it is confirmed that the ASI-Gauss technique is an efficient method for analyses of frame structures both in elastic and plastic range, and even the two-element modeling is sufficient to acquire the results with high accuracy and reliability.

3.3 Impact analysis of a simple two-beam model

In this section, impact phenomenon of two beams is simulated to verify the creditability of the elemental contact algorithm. The analyzed model, its geometrical properties and material constants are shown in Fig.10. One of the beams is fixed at its both ends while the other one moves freely. Initial velocity of 50 m/s is applied to the free beam. The beams are modeled with two elements per each member. The ASI-Gauss technique is applied, and the updated Lagrangian formulation (ULF) is used since large deformations are expected in the analysis. Damping effect is not considered in the analysis. The time increment Δt is set to 10 μs. The calculation is done for a total of 3000 steps (0.03 s).

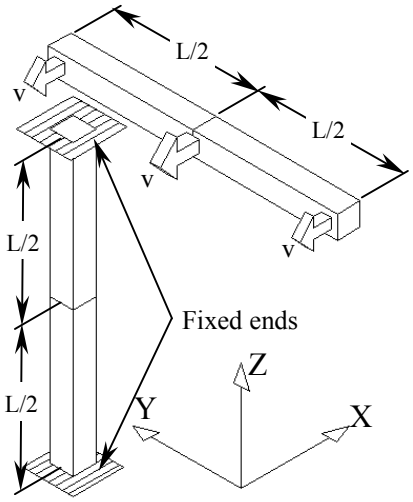

$L = 1.00\ \text{m},\ v = 50\ \text{m/s}$

$A = 2.50 \times 10^{-3}\ \text{m}^2$

$I_x = I_y = 5.21 \times 10^{-7}\ \text{m}^4$

$\rho = 7900\ \text{kg/m}^3,\ E = 206\ \text{GPa}$

$\upsilon = 0.3,\ \sigma_y = 245\ \text{MPa}$

$M_{x0} \equiv M_{y0} = 7.66 \times 10^3\ \text{Nm}$

$N_0 = 6.13 \times 10^5\ \text{N},\ M_{z0} = 1.12 \times 10^5\ \text{Nm}$

Figure 10: Analyzed two-beam model.

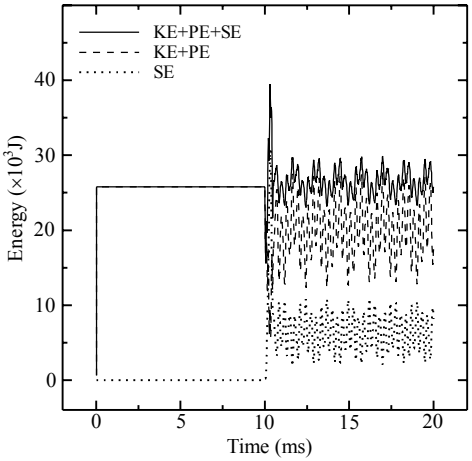

Figure 11: Kinetic, potential and strain energies in the two-beam model.

Figure 11 shows the sum of kinetic and potential energies, strain energy and the total of all three for the whole model. Energies for both the colliding and the fixed beams constituted by a total of four elements are calculated by using the following equations:

$$KE = \frac{1}{2}\sum_{i=1}^{4}\rho A\frac{l_i}{2}\left(v_{i1}{}^2 + v_{i2}{}^2\right) \tag{20a}$$

$$PE = \sum_{i=1}^{4}\rho A\frac{l_i}{2}g\left(h_{i1} + h_{i2}\right) \tag{20b}$$

$$SE = \frac{1}{2}\sum_{i=1}^{4}\{\sigma_i\}\{\varepsilon_i\}l_i \tag{20c}$$

Here, KE, PE and SE stand for kinetic energy, potential energy and strain energy, respectively. $\{\sigma_i\},\{\varepsilon_i\}$, h_i, l_i represent the resultant force vector, the generalized strain vector, z coordinates and the length of the element E_i (i=1,2,3,4). Subscripts 1 and 2 denote the nodal points of the corresponding element.

As seen from the figure, kinetic and potential energies occupy all of the total energy before the impact takes place. After the impact, both beams deflect and vibrate as seen in Fig.12. As a consequence, the strain energy is stored up in the beams and the sum of the other two

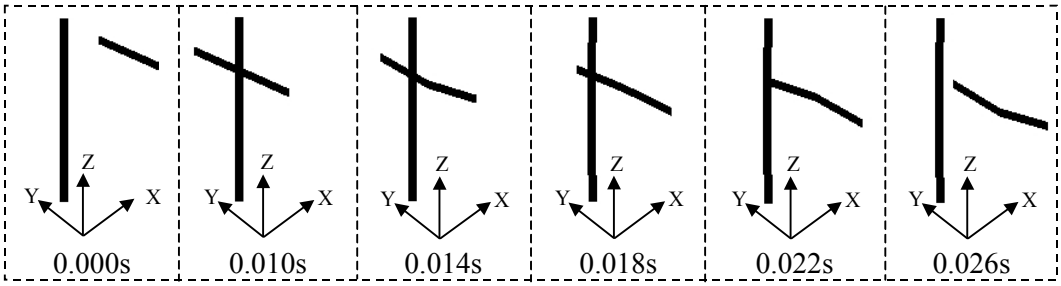

Figure 12: Impact analysis of a simple two-beam model.

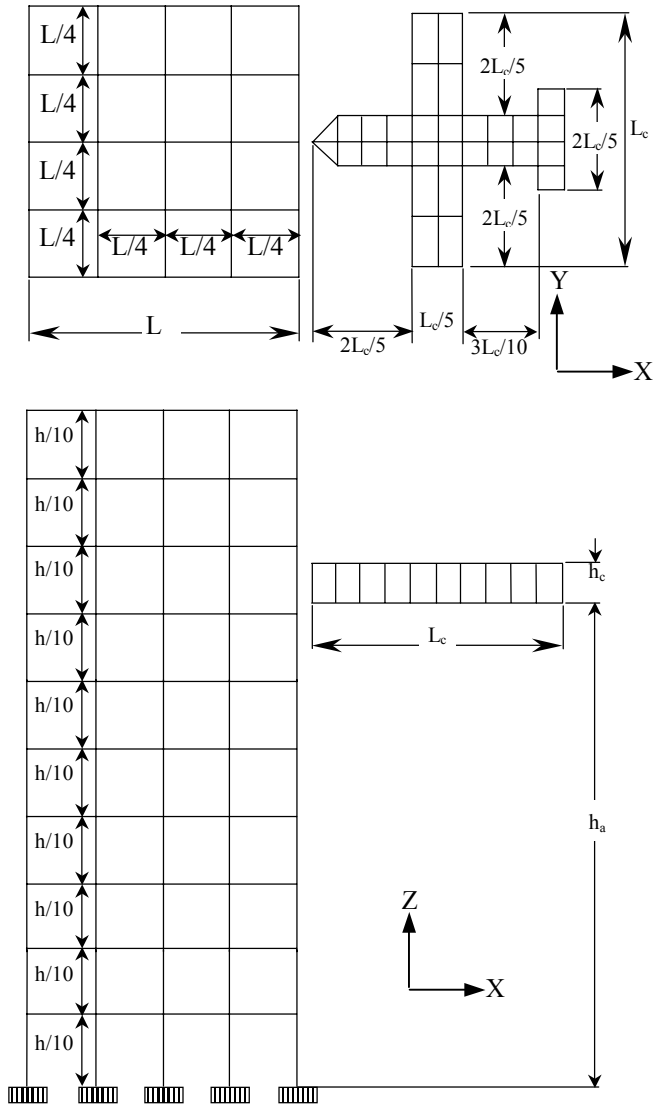

	Body 1	Body 2	Unit
L	16	-	m
L_c	-	15	m
h	30	-	m
h_c	-	2	m
h_a	-	21.50	m
A	2.19×10^{-2}	1.00×10^{-2}	m^2
I_x	6.66×10^{-4}	8.33×10^{-6}	m^4
I_y	2.24×10^{-4}	8.33×10^{-6}	m^4
ρ	7900	2800	kgm^{-3}
E	206	69	Gpa
σ_y	240	195	Mpa
ν	0.30	0.335	
M_{xo}	7.99×10^{5}	4.88×10^{4}	Nm
M_{yo}	2.69×10^{5}	4.88×10^{4}	Nm
N_o	5.25×10^{6}	1.95×10^{6}	N
M_{zo}	1.12×10^{5}	1.12×10^{5}	Nm

Body 1: Ten-storied steel framed structure
Body 2: Aircraft (made of duralumin)

Figure 13: Analyzed ten-storied steel framed structure and the aircraft.

decreases. The main reason for the fluctuations seen after the impact is considered to be the occurrence of longitudinal and bending waves. However, the total energy remains almost constant, and the elemental contact algorithm used in this study is considered to be sufficiently reliable.

4 STRUCTURAL COLLAPSE ANALYSIS OF FRAMED STRUCTURES UNDER IMPACT LOADS

In this section, dynamic collapse analyses are performed using the ASI-Gauss technique to simulate the impact of a small aircraft into a ten-storied steel framed structure. A total of four cases are analyzed using different values for three parameters: cruise speed, size and weight

of the aircraft. Details of the analyzed model, propagation of impact loads, response of the structures and the extent of impact damage are discussed in this section.

4.1 Outline of the analyzed model

Figure 13 shows the analyzed ten-storied framed structure and the aircraft. Both structures are modeled by using two elements per each member. The model contains 1698 elements and 7308 degrees of freedom. The gap elements, which bind the elements in contact for a certain period of time, are assumed to have the same geometrical and material properties as the elements forming the aircraft. The critical values for bending strain and axial strain are set to $\kappa_{fx}=\kappa_{fy}=0.04$ and $\varepsilon_{fz}=0.3$ in these analyses.

The weight of the floor system is considered and nearly twenty times of the own weight of the skeletal structure is applied as dead loads. The ten-storied framed structure is fixed at its lower ends while none of the element is fixed in the aircraft model. It is assumed that the total weight of the aircraft is uniformly distributed in its elements. Initial velocity is applied to the aircraft with zero degree of inclination from the horizon.

4.2 Parameters set in the analyses

A total of four analyses are performed using different values for cruise speed, size and weight of the aircraft. The combinations of these parameters are shown in Table 1. The parameters are selected to fix the pre-impact kinetic energy values for Cases I and IV, Cases II and III to be the same. In all the four analyses, the ASI-Gauss technique with the linear Timoshenko beam element is used and member fracture and elemental contact are both considered. Damping effect is not considered in all analyses. The updated Lagrangian formulation (ULF) is used to handle large deformations of the elements. The Conjugate Gradient (CG) method is used as the solver to reduce the need for memory resources. For Newmark's β method [9], 1/6 to 1/4 is the commonly used range for β. However, it is known that it becomes less precise but more stable with a value of β between 1/4 and 1/2. Since strongly nonlinear and discontinuous behaviors of the problem in this study cause instability in calculations, we used a value of 0.4 for β. The time increment Δt is set to 10 μs. The calculation is done for a total of 35000 steps (0.35 s) for each case. The calculation for each case takes approximately 20 CPU hours with a personal computer (2.4 GHz CPU, 256 MB RAM).

4.3 Structural collapse analysis of the ten-storied framed structure under impact loads

Figure 14 shows the results of the first analysis (Case I). A total of six colors are used to

Table 1: Parameters of the aircraft

Case No.	Cruise speed [kmph]	Size L_c [m]	Weight [kg]	Pre-impact kinetic energy [J]
Case I	440	15	60000	448 x10^6
Case II	311	15	60000	224 x10^6
Case III	440	15	30000	224 x10^6
Case IV	440	12	60000	448 x10^6

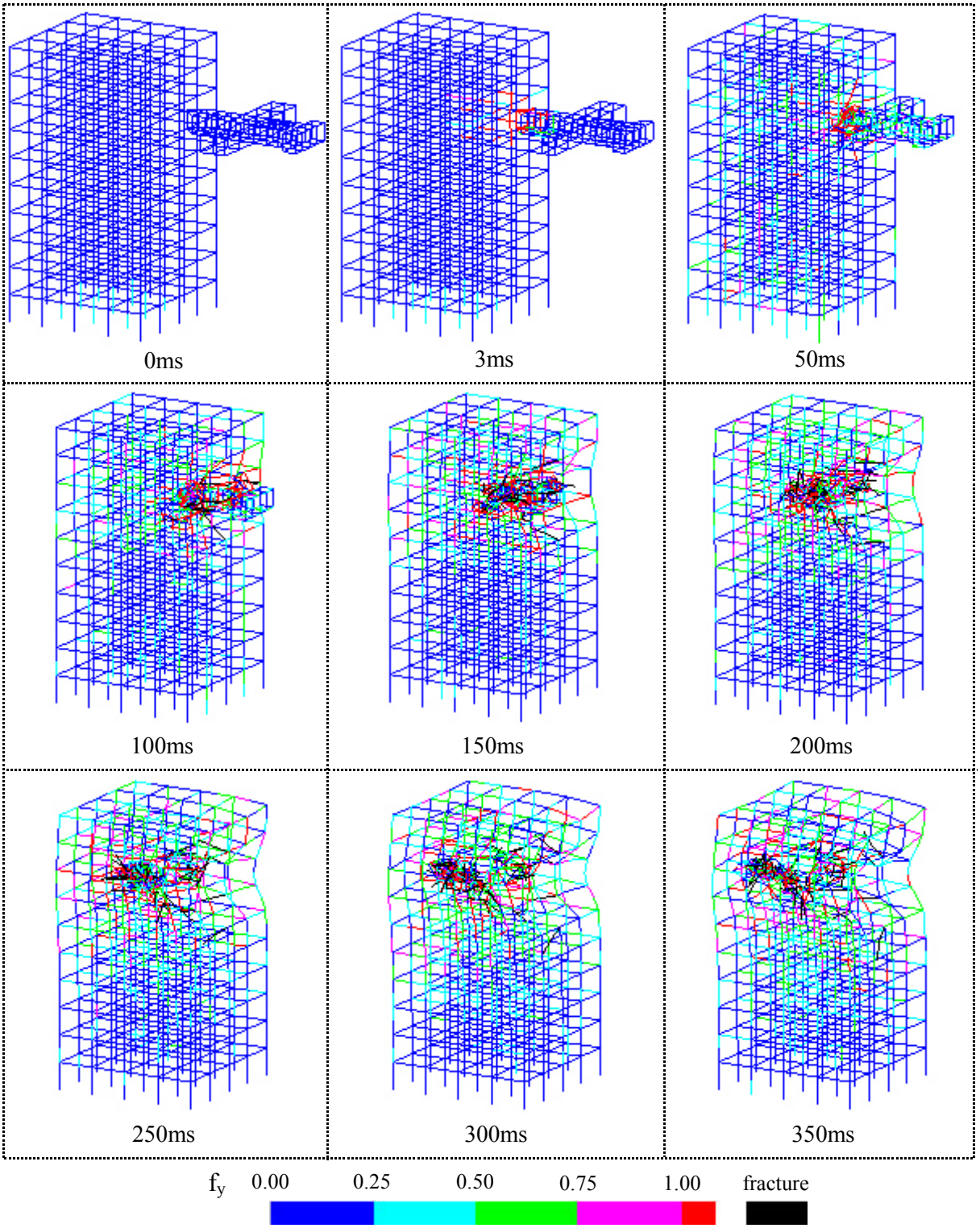

Figure 14: Impact analysis of a ten-storied framed structure collided by a small aircraft (Case 1).

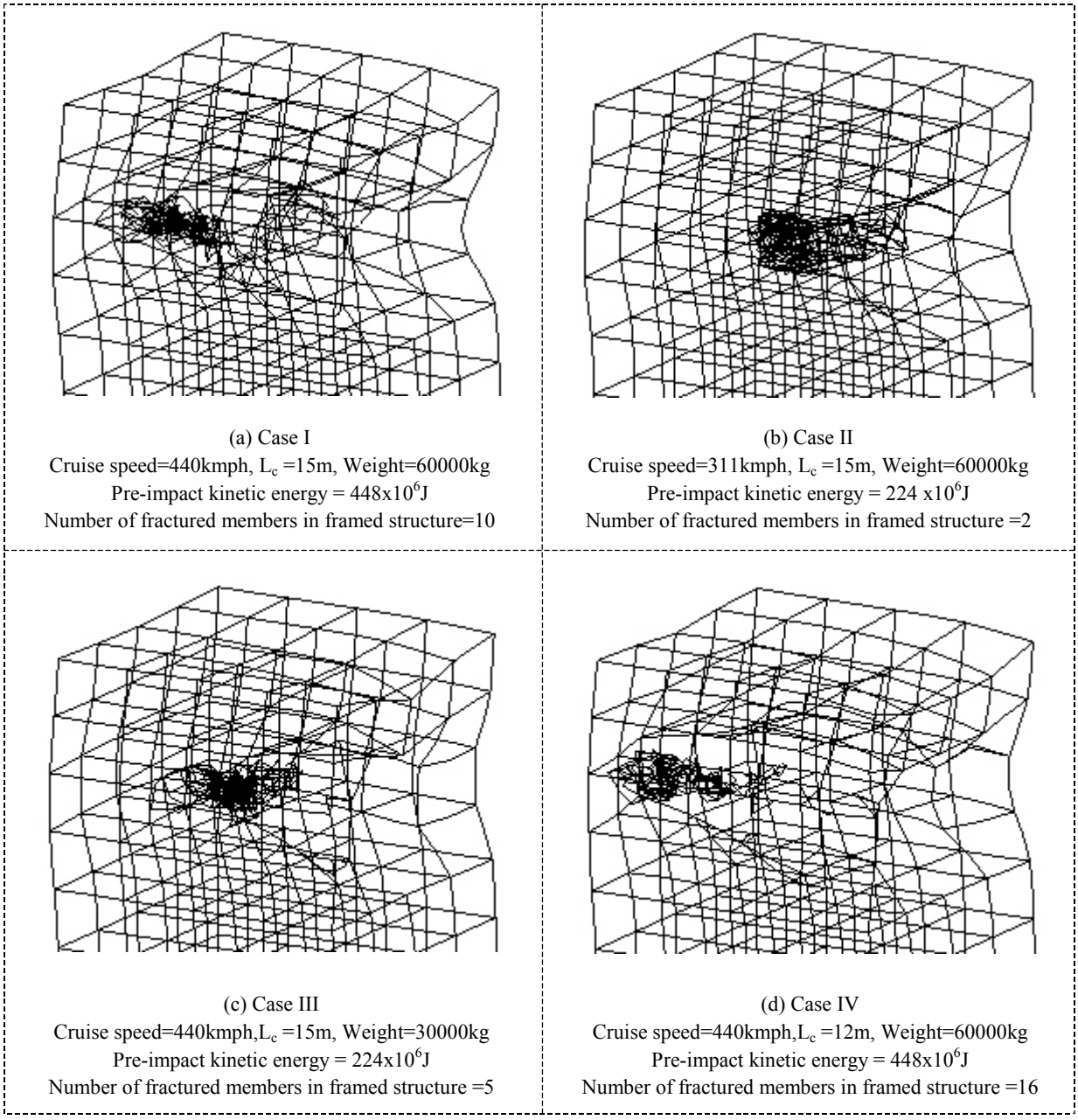

(a) Case I
Cruise speed=440kmph, L_c =15m, Weight=60000kg
Pre-impact kinetic energy = 448×10^6J
Number of fractured members in framed structure=10

(b) Case II
Cruise speed=311kmph, L_c =15m, Weight=60000kg
Pre-impact kinetic energy = 224×10^6J
Number of fractured members in framed structure =2

(c) Case III
Cruise speed=440kmph,L_c =15m, Weight=30000kg
Pre-impact kinetic energy = 224×10^6J
Number of fractured members in framed structure =5

(d) Case IV
Cruise speed=440kmph,L_c =12m, Weight=60000kg
Pre-impact kinetic energy = 448×10^6J
Number of fractured members in framed structure =16

Figure 15: Impact damage to the ten-storied framed structure (only the upper five floors are shown and fractured elements are excluded).

demonstrate the tendency of the elements to yield or fracture. The numbers in the color palette indicate the values of f_y in Eq. (14). Red color (f_y =1.0) means a plastic hinge is formed within the element and black color is used for fractured elements.

Propagation of impact loads can be confirmed by observing the spread of colors in the figure. Immediately after the impact, red color propagates into the structures from the point of

impact. The elements near the area of impact turn to black, that is, they start to fracture. Moreover, it is seen that the colors travel down the columns and move backwards very fast. This phenomenon is seen mainly in the columns and considered as the propagation of shock waves. Red-colored elements are temporarily found even in the lowest floor, and this means that even the lowest floor is affected, to some extent, by the impact.

Figures 15(a) to 15(d) show the extent of damage to the steel framed structure for all four cases. In order to show the damaged areas clearly, only the upper five floors are plotted and the fractured elements are excluded. If we focus on Case I (Fig.15(a)) and II (Fig.15(b)), the impact damage is seen larger in Case I in which the cruise speed of the aircraft is larger (and so is the pre-impact kinetic energy), and most parts of the aircraft penetrate the framed structure. Although the pre-impact kinetic energy of Case II and III (Fig.15(c)) are the same, the results show a slight difference between the damage patterns. If we compare the results between Case I and IV (Fig.15(d)), where the only difference between the two cases are the width of the aircraft, we can see that the shorter the width, the deeper the penetration. In Case IV, most of the inner columns are cut off, however, the total deformation of the framed structure is observed slightly smaller than in Case I. This result can be interpreted in such a way that the size of the aircraft has a strong influence on the damage patterns. Moreover, soon after impact in Case I, tensile stresses are observed in the columns that had been compressed by gravity loads before impact as shown in Fig.16. There is a possibility that these tensile stresses lead to some degree of structural damage especially in the joints of beams and columns. Therefore, further detailed analyses are necessary to investigate this phenomenon.

5 CONCLUSION

The formerly developed ASI technique for the linear Timoshenko beam element provides higher computational efficiency than the conventional finite element scheme, and is known to be able to cope with dynamic behaviors with strong nonlinearities including such phenomena as member fracture. However, it still lacked accuracy in elastic range when the number of elements per member is small. In this study, the ASI-Gauss technique, which deals elastic members by locating the stress evaluation points of two consecutive elements at Gaussian points, is proposed. Elasto-plastic analyses under both static and dynamic loading are performed to verify the proposed technique, and it is confirmed that nearly converged solutions are obtained even when the number of elements per member is two. It gives results with high accuracy at very low calculation cost, which may act efficiently in application to analyses of large-scale framed structures.

Instead of applying impact loads in the form of nodal forces, impact phenomenon is simulated by means of contacts between the elements involved. This elemental contact algorithm is also useful to simulate fractured elements colliding with other elements, and to consider the variation of parameters of the colliding structure. The elemental contact algorithm is verified from the point of conservation of energy and the result showed its high reliability.

The ASI-Gauss technique with the elemental contact and the member fracture algorithms are applied to dynamic analyses with strong nonlinearities and discontinuities, where impact

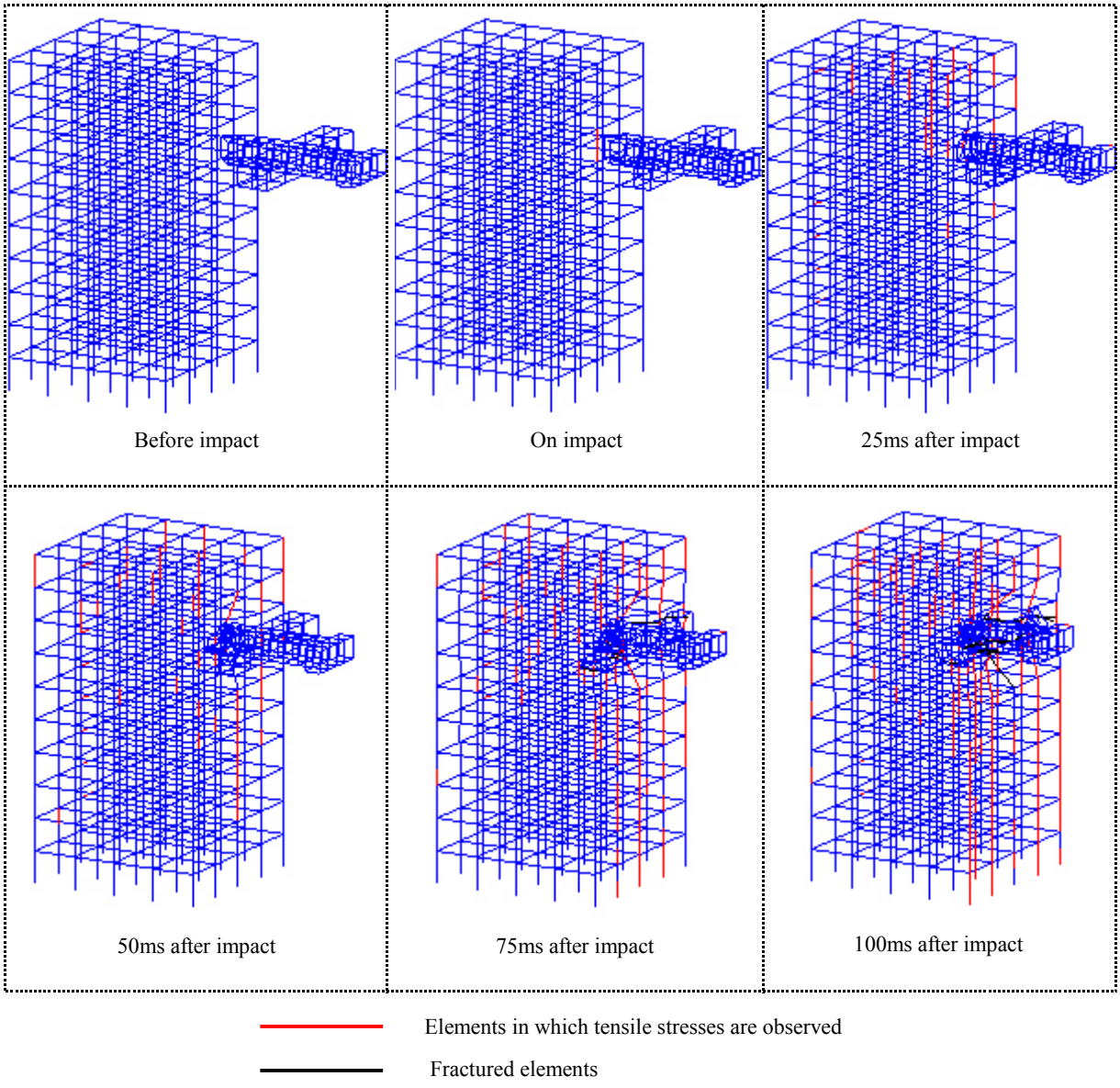

Figure 16: Tensile stresses observed in the ten-storied framed structure after impact (Case I).

of an aircraft against a ten-storied framed structure is discussed using four different sets of parameters for the aircraft. From the results, we observed the propagation phenomenon of impact loads and shock waves. Also, a proper difference in impact damage is obtained by different sets of parameters, and in practically short calculation time. Therefore, the numerical analysis code used in this study is considered to be an efficient code for impact analyses of large-scale framed structures. However, further study is considered necessary to evaluate the structural damage caused by the tensile stresses of the columns, and damping matrices as well as the wall and floor slabs should also be considered in the future to improve the accuracy.

REFERENCES

[1] P.A. Cundall. A Computer Model for simulating Progressive, Large-scale Movement in Blocky Rock System. *Proceedings of the International Symposium on Rock Mechanics*, **II-8**, 129-136, 1971.

[2] G.H. Shi and R.E. Goodman. Discontinuous Deformation Analysis. *Proceedings of 25th U.S. Symposium on Rock Mechanics*, 269-277, 1984.

[3] H. Tagel-Din and K. Meguro. Nonlinear Simulation of RC Structures Using Applied Element Method. *Structural Engineering / Earthquake Engineering*, **17(2)**, 137-148, 2000.

[4] Y. Toi and D. Isobe. Adaptively Shifted Integration Technique for Finite Element Collapse Analysis of Framed Structures. *Int. J. Numer. Methods Eng.*, **36**, 2323-2339, 1993.

[5] Y. Toi and D. Isobe. Finite Element Analysis of Quasi-static and Dynamic Collapse Behaviors of Framed Structures by the Adaptively Shifted Integration Technique. *Computers and Structures*, **58(5)**, 947-955, 1996.

[6] D. Isobe and Y. Toi. Analysis of Structurally Discontinuous Reinforced Concrete Building Frames Using the ASI Technique. *Computers and Structures*, **76(4)**, 471-481, 2000.

[7] D. Isobe and M. Tsuda. Seismic Collapse Analysis of Reinforced Concrete Framed Structures Using the Finite Element Method. *Earthquake Engineering and Structural Dynamics*, **32(13)**, 2027-2046, 2003.

[8] W.H. Press, S.A. Teukolsky, W.T. Vetterling, B.P. Flannery. *Numerical Recipes in FORTRAN: The Art of Scientific Computing*, 2nd ed. Cambridge University Press, 1992.

[9] N.M. Newmark. A Method of Computation for Structural Dynamics. *A.S.C.E. J. Engineering Mechanics*, **85**, 67-94, 1959.